Lab on a Chip

Accepted Manuscript

ROYAL SOCIETY OF CHEMISTRY

www.rsc.org/loc

Detaching droplets in immiscible fluids from a solid substrate with help of electrowetting

Jiwoo Hong and Sang Joon Lee*

Center for Biofluid Flow and Biomimic Research

Department of Mechanical Engineering, Pohang University of Science and Technology,

San 31, Hyoja-dong, Pohang 790-784, South Korea

*Corresponding author. Tel.: +82-54-279-2169; fax: +82-54-279-3199.

E-mail address: sjlee@postech.ac.kr.

Abstract

The detachment (or removal) of droplets from a solid surface is an indispensable process in numerous practical applications which utilize digital microfluidics, including cell-based assay, chip cooling, and particle sampling. When a droplet that is fully stretched by impacting or electrowetting is released, the conversion of stored surface energy to kinetic energy can lead to the departure of the droplet from a solid surface. Here we firstly detach sessile droplets in immiscible fluids from a hydrophobic surface by electrowetting. The physical conditions for droplet detachment depend on droplet volume, viscosity of ambient fluid, and applied voltage. Their critical conditions are determined by exploring the retracting dynamics for a wide range of driving voltages and physical properties of fluids. The relationships between physical parameters and dynamic characteristics of retracting and jumping droplets, such as contact time and jumping height, are also established. The threshold voltage for droplet detachment in oil with high viscosity is largely reduced (~70%) by electrowetting actuations with a

square pulse. To examine the applicability of three-dimensional digital microfluidics (3D-DMF) platforms to biological applications such as cell culture and cell-based assays, we demonstrate the detachment of droplets containing a mixture of human umbilical vein endothelial cells (HUVECs) and collagen (concentration of 4×10^4 cells/mL) in silicone oil with a viscosity of 0.65 cSt. Furthermore, to complement the technical limitations due to the use of a needle electrode and to demonstrate the applicability of the 3D-DMF platform with patterned electrodes to chemical analysis and synthesis, we examine the transport, merging, mixing, and detachment of droplets with different pH values on the platform. Finally, by using DC and AC electrowetting actuations, we demonstrate the detachment of oil droplets with very low contact angle (< ~13°) in water on a hydrophobic surface.

Introduction

Detachment of droplets from a solid surface is one of the essential and crucial processes in numerous practical applications in the field of digital (or droplet-based) microfluidics (DMF),[1-3] including cell culture,[4-8] electronic cooling,[9,10] cleaning and sampling of microparticles.[11-13] Several methods for detaching droplets from a solid surface have been proposed; examples of these methods include mechanical vibration,[14,15] electrostatic forces,[16–18] and nanoparticle suspensions.[19–21] However, these methods have technological problems, such as noise generation and difficulty in integration due to mechanical moving parts, high voltage (~a few kV) or high electric field (~MVm^{-1}), and the addition of surfactant or nanoparticles.

Recently, electrowetting (EW) has been introduced as an alternative method to alleviate these technical problems.[22–25] EW is a technique that electrically controls the

wettability of a droplet on the substrate. This technique has several advantages, including fast response, low driving voltage, and absence of mechanically moving parts.[26] Lee et al. observed that a droplet is continuously bounced on the superhydrophobic surface by using AC EW at the resonance frequency.[22] They also reported that a droplet can jump on the superhydrophobic surface by EW actuations with square pulses as well as sinusoidal pulses.[23] Recently, Lapierre et al. demonstrated that a droplet can be bounced on the superhydrophobic surface by applying AC modulated signal.[24] More recently, we extended previous studies on the detachment of droplets from superhydrophobic surfaces[22-24] by demonstrating the EW-induced droplet detachment from a hydrophobic surface with the applied square pulses.[25] The development of these methods for droplet detachment by using EW could lay the foundation for the construction of three-dimensional DMF (3D-DMF) platforms. We believe that 3D-DMF will resolve the problems of existing two-dimensional DMF (2D-DMF) systems, including cross-contamination[27] and solute adsorption[28] as well as the requirements for high-density device-integration.

However, the droplet detachment methods proposed by previous studies[22-25] were tested in air media. In the construction of 3D-DMF platforms, the aforementioned methods have some technical issues such as high driving voltage requirement and difficulty in droplet manipulation at a high temperature due to evaporation. These issues can be resolved by introducing an immiscible fluid (e.g., water–oil) system. For instance, the oil medium reduces contact-angle hysteresis and lowers the driving voltage.[1,29,30] The medium also prevents droplet evaporation, thus allowing the droplet to be manipulated at a high temperature.[1,31] In addition, the oil medium inhibits surface contamination caused by the adsorption of biomolecules.[32,33] Accordingly, it is required to extend previous researches on the detachment

of droplets in air medium[22-25] by the demonstrating EW-induced droplet detachment in immiscible fluids. In this study, we firstly demonstrate that sessile droplets in submerged immiscible fluids (i.e., water droplets in oil and oil droplets in water) can be detached from a hydrophobic surface by simple DC EW actuations. To find the critical physical conditions and dynamic characteristics (e.g., contact time and jumping height) for droplet detachment in oil media, the retracting and jumping behaviors of sessile droplets submerged in oil are explored under varying physical conditions of applied voltage, droplet volume, and oil viscosity when the electrowetted droplets are released (i.e., the applied DC voltage is turned off). In addition, contact time and jumping height as a function of aforementioned parameters are determined. To reduce the threshold voltage for detaching droplets in oil with high viscosity, the EW actuation with a square pulse is also employed. To get closer to the realization of the 3D-DMF platform for cell culture and cell-based assays, we examine the detachment of droplets containing a mixture of human umbilical vein endothelial cells (HUVECs) and collagen. Moreover, as a basic application of the 3D-DMF platform with patterned electrodes for chemical analysis and synthesis, we examine the transport, merging, mixing, and detachment of droplets with different pH values on patterned electrodes. Finally, we demonstrate the detachment of oil droplets in water from a hydrophobic surface by using DC and AC EW actuations.

Materials and methods

The experimental setup employed in this study [Fig. 1(a)] is similar to a typical apparatus used for the EW experiment in oil medium.[34] The indium tin oxide electrode plate is coated with a dielectric layer (parylene-C, 5 μm thickness) and a hydrophobic layer

(DuPont, AF1600® with 100 nm thickness), which is combined with a transparent acrylic cell (6 cm length, 3 cm width, and 2 cm height). The cell is filled with silicone oil (Shin-Etsu Silicone Korea Co., Ltd.) as non-conducting liquid, which has kinematic viscosities of 0.65 cSt and 5 cSt. The conducting liquid is an aqueous 0.1 M NaCl solution. The interface tension between the saline solution and silicone oil is measured by using an EW-based tensiometer method (Fig. S1 in the Supplementary Information).[34,35] The measured interfacial tensions are 0.020 N/m and 0.023 N/m for silicone oils with viscosities of 0.65 cSt and 5 cSt, respectively. These values are in good agreement with those previously reported.[36] The data provided by the supplier show that densities of the tested silicone oils with viscosities of 0.65 cSt and 5 cSt are 0.76 g/mL and 0.92 g/mL, respectively. The corresponding variations in interface tension and density remain small. A droplet of saline solution with volumes ranging from 0.5 μL to 15 μL is dispensed with a micropipette onto the hydrophobic surface.

To demonstrate the detachment of droplets containing biochemical sample, a mixture of human umbilical vein endothelial cells (HUVECs) and collagen is used. Here, we briefly summarize the preparation procedure of the mixture. More detailed information is available in references 36 and 37. HUVECs (Invitrogen, Carlsbad, CA, USA) are cultured in Medium 200 (Gibco) with low-serum growth supplement (Gibco) containing 20% fetal bovine serum (Gibco) and 1% penicillinstreptomycin (HyClone) under a humidified atmosphere of 5% CO_2 at 37°C. The HUVECs are washed with Dulbecco's phosphate buffered saline (DPBS) and detached from the flask with trypsin–EDTA solution. The detached cells are then pelleted by slow centrifugation and resuspended in Medium 200 solution. To prepare the HUVECs mixed with collagen, 3 mg/mL collagen type I (from rat tails; Invitrogen, Carlsbad, CA, USA) is diluted to a final concentration of 1 mg/mL by using

DPBS solution containing calcium and magnesium. The HUVECs suspension and collagen are mixed with the volume ratio of three to one at 4°C. Consequently, the mixture of HUVECs and collagen has a concentration of 4×10^4 cells/mL.

A tungsten wire with a diameter of 25 μm is immersed in the test droplet as a top electrode. Our previous studies confirmed that the EW dynamics of a droplet is rarely affected by needle electrode.[36,39] Electrical signals produced by a function generator (33220A, Agilent) and amplifier (A800, FLC) are applied between a tungsten wire and an electrode plate. In this study, the dimensionless EW number $\eta = \varepsilon_d\varepsilon_o V^2/2d\gamma$ is used as one of the governing parameters instead of applied voltage. It represents the relative strength of electrostatic energy compared to surface tension.[26] Here, ε_d and d are the dielectric constant and thickness of insulator, ε_o the vacuum dielectric permittivity, V the applied voltage, and γ the interfacial tension between liquids. To evaluate the EW number, the values of ε_d= 3.1, ε_o= 8.854×10^{-12} F/m, and d= 5 μm are used. The retracting and jumping phenomena of the electrowetted droplets are recorded consecutively with a high-speed camera (Fastcam SA3, Photron) at a frame rate ranging from 2,000 fps to 4,000 fps depending on the contact-line speed. Digital image processing and data analysis are conducted using both MATLAB® and a public-domain image-processing program (ImageJ, NIH).

Results and discussion

The effect of applied voltage on the detachment process is explored by observing the retracting and jumping behaviors of 5 μL droplets in silicone oil with a viscosity of 0.65 cSt when the electrowetted droplet at different η is released [Figs. 1(b)–(d)]. The temporal variations of the shape of retracting droplets with low and high η conditions are shown in Fig.

1b. The effect of applied voltage on the retracting and jumping dynamics is quantified by measuring the temporal evolutions of the base radius [Fig. 1(c)] and the dimensionless height [Fig. 1(d)]. Here, dimensionless height ($\tilde{H}$) is defined as the apex height (H_{apex}) divided by the diameter of a spherical droplet of the same volume, $D = (6\Delta/\pi)^{1/3}$, where Δ is the droplet volume. Droplet jumping phenomena are observed when η is larger than 0.34, which corresponds to the applied voltage of 50 V. For 5 μL droplets in air, the threshold values of η for cases of single and double square pulse actuations are η= 0.6–0.1 and 0.4–0.1, respectively.[25] Thus, the oil medium can be used to reduce driving voltage for droplet detachment. The contact-line speed of the retracting droplet is estimated from the slope of Fig. 1(c) (Fig. S2 in the Supplementary Information). On the one hand, the contact-line speed of the retracting droplet when η is larger than 0.34 increases largely in the very early stage (approximately up to 1 ms) and then decreases in the subsequent stage (approximately up to 10 ms). Thereafter, the contact-line speed increases again, eventually allowing the droplet to jump. On the other hand, contact-line speed when η is smaller than 0.34 slightly increases in the very early stage (approximately up to 1 ms) and then remains almost constant.

The relationships between applied voltage and the dynamic characteristics of retracting and jumping droplets, such as contact time (i.e., time elapsed to reach before jumping) and jumping height, are established. The maximum dimensionless height $\tilde{H}_{max}$ has a power-law dependence on the EW number, $\tilde{H}_{max} \propto \eta^{0.4}$ (Fig. 1e). It is approximately linearly proportional to the applied voltage. The maximum height is almost saturated when η is larger than 1.66. As the applied voltage increases, the radius and surface energy of the electrowetted droplet also increase. That is, the droplet with large surface energy can be detached from the substrate and jump higher than that with low surface energy. The time

elapsed to reach the maximum dimensionless height is found to be approximately 0.6th power of η (Fig. S3 in the Supplementary Information).

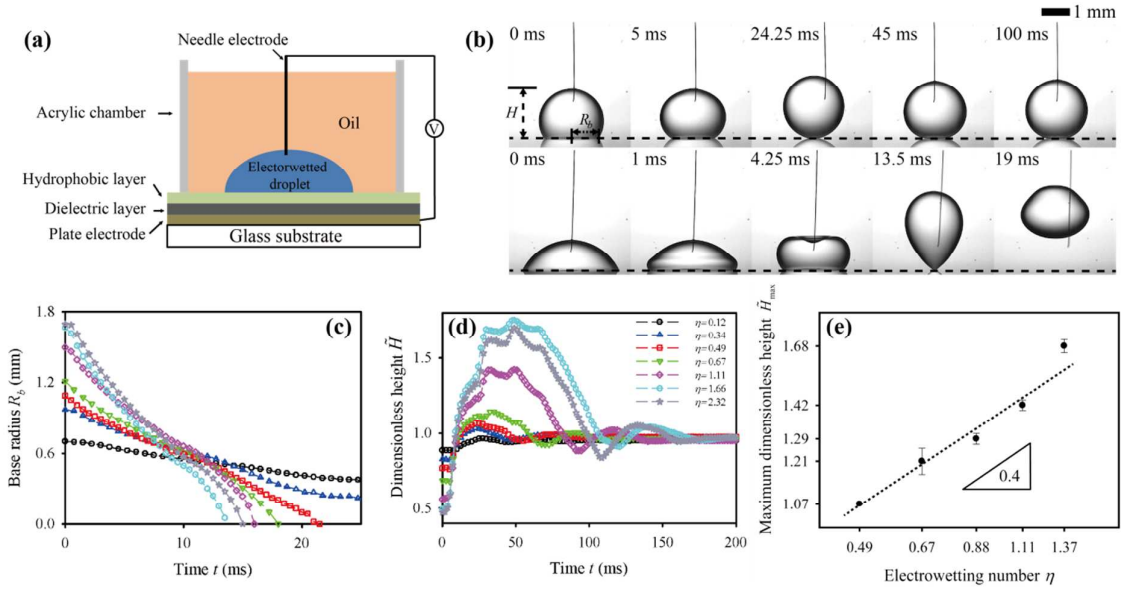

Fig. 1 Effect of applied voltage on droplet detachment. (a) Schematic diagram of the experimental setup. (b) Temporal shape variations of retracting 5 μL droplets in ambient oil with a viscosity of 0.65 cSt at η = 0.34 (top) and η = 1.66 (bottom). Dashed lines indicate the contact surface of the droplet. (c) and (d) Temporal variations of base radius (R_b) and dimensionless height ($\tilde{H}$), respectively, during the retracting and jumping processes of droplets at different EW numbers. (e) Power-law dependence of the maximum dimensionless height (H_{max}/D) of jumping droplets on EW number η (log-log scale). The error bar denotes the standard deviation. The triangular inset shows that the maximum dimensionless height is proportional to the 0.4th power of EW number η (regression $R^2 = 0.974$).

Non-dimensional analysis is carried out for the data in Fig. 1(c) to effectively characterize the retracting dynamics of jumping droplets. In the present study, a relaxation time as a characteristic time scale is derived from energy balance between the stored energy of the electrowetted droplet (ΔE) and the kinetic energy $E_{kinetic} = \rho\Omega U^2 / 2$, where, ρ and Ω denote the density and volume of the droplet, and U the velocity of the retracting droplet. Since ΔE is equal to the electric energy $E_{el} = \gamma S\eta$ imparted by the applied voltage (Supplementary Information), the following relationship can be obtained: $\gamma S\eta = \rho\Omega U^2 / 2$, where S denotes the contact area between the droplet and solid substrate. When S, Ω, U are scaled as R^2, R^3, and R/τ, respectively, the relaxation time can be expressed as $\tau \sim (\rho R^3/\eta\gamma)^{0.5}$, where R is the initial base radius as a characteristic length. More detail information on the relaxation time is well described in the Supplementary Information. When the time and length scales are nondimensionalized by the relaxation time and the initial base radius, respectively, almost all the data collapse into one curve along the time axis [Fig. 2(a)]. The merged data depicted in Fig. 2(a) shows that contact time is mainly governed by a relaxation time and is inversely proportional to the 0.5th power of EW number. This tendency is also obtained from the contact time measured experimentally at different EW numbers [Fig. 2(b)].

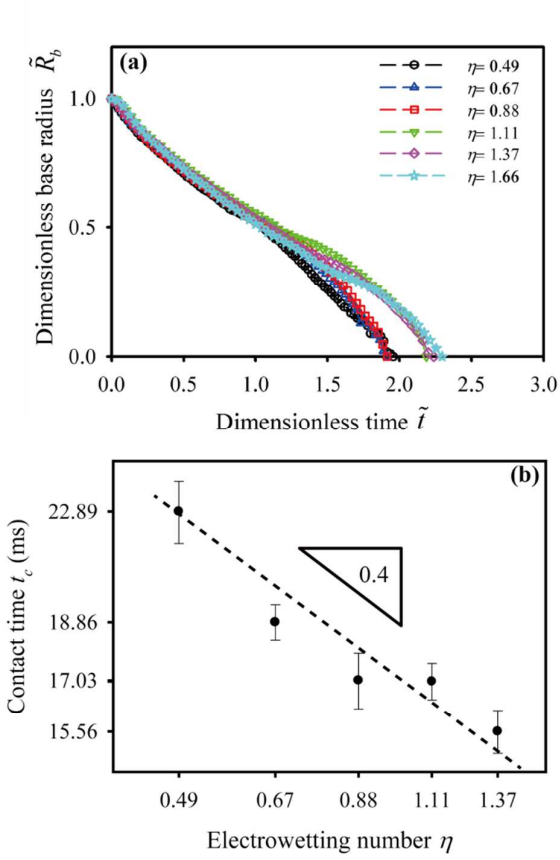

Fig. 2 Effect of applied voltage on the contact time. (a) Rescaling of the plot of Fig. 1(c) by using a relaxation time ($\tau \sim (\rho R^3/\eta\gamma)^{0.5}$), ρ: droplet density, R: radius of a spherical droplet, and γ: interfacial tension) and initial radius. (b) Power-law dependence of the contact time of rectracting 5 μL droplets in silicone oil with a viscosity of 0.65 cSt on the EW number η. Note that both x and y axes are logarithmic scales.The error bar denotes the standard deviation. The triangular inset shows that the contact time for detaching the droplet is approximately inversely proportional to the 0.4 power of η (regression R^2= 0.915).

The effect of droplet volume on the detachment process is explored by quantitatively analyzing the temporal variations of the base radius and apex height of droplets with volumes ranging from 0.5 μL to 15 μL at a fixed η of 1.37 [Figs. 3(a) and (c)]. Both retracting and jumping behaviors exhibit qualitatively similar patterns regardless of droplet volume. When

the time and length scales in Fig. 3(a) are also nondimensionalized by a relaxation time (τ) and initial base radius, respectively, almost all the data in Fig. 3(a) collapse into one curve along the time axis [Fig. 3(b)]. That is, contact time is mainly governed by the relaxation time and is proportional to the 0.5th power of droplet volume. This relationship is also obtained from the contact time measured experimentally at different droplet volumes (Fig. S6 in the Supplementary Information). In addition, this relationship is similar to that found in previous reports on droplet impact in air medium.[40]

A relationship between droplet volume and threshold voltage (or EW number) is also established. When droplet volumes vary from 1 μL to 10 μL, the threshold values of η are within the range of η = 0.30–0.43 (50 V to 60 V). When the droplet volume increases to 13 μL and 15 μL, the threshold values of η shift toward the high range of η = 0.43–0.58 (60 V to 70 V). Although the threshold value for each droplet volume is slightly different, all droplets are situated in the range of η = 0.30–0.58 (50 V to 70 V). Consequently, threshold voltage is rarely affected by droplet volume. This result is similar to that found in our previous work on droplet detachment in air medium.[25] In addition, $\tilde{H}_{max}$ tends to slightly decrease as the droplet volume increases, but a certain relationship between them cannot be established [Fig. 3(d)].

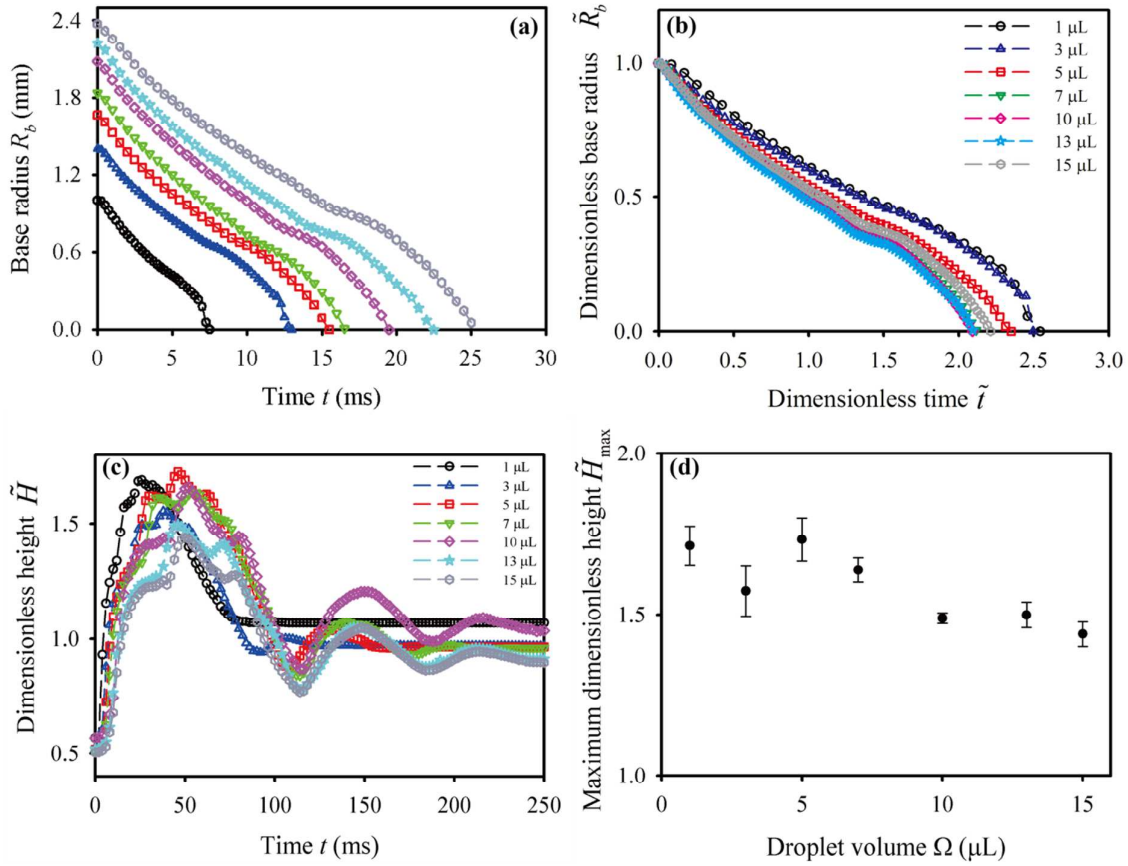

Fig. 3 Effect of droplet volume on droplet detachment. (a) Temporal variations of base radius during the retracting and jumping behaviors of droplet. (b) Rescaling of the plot of (a) by using a relaxation time ($\tau \sim (\rho R^3/\eta\gamma)^{0.5}$) and initial radius. The merged data in (b) show that contact time is mainly governed by a relaxation time. (c) Temporal variations of dimensionless height ($\tilde{H}$). (d) Relationship between maximum dimensionless height of jumping droplets and droplet volume. Note that both x and y axes are linear scales. The maximum dimensionless height $\tilde{H}_{max}$ tends to slightly decrease as the droplet volume increases. However, a certain relationship between them is not established.

The detaching droplets in oil with a high viscosity of 5 cSt are investigated by measuring the temporal variations of the base radius [Fig. 4(a)] and dimensionless height [Fig. 4(b)] during the retracting and jumping processes of droplets at different η. In oil with high viscosity of 5 cSt, droplet jumping is observed when η is larger than 1.19, which corresponds to the applied voltage of 100 V. This threshold voltage is about twice that in oil with a low viscosity of 0.65 cSt. In addition, the maximum height of a jumping droplet in oil with a high viscosity of 5 cSt is smaller than that in oil with a low viscosity of 0.65 cSt.

Besides the aforementioned parameters, the wetting properties of a solid surface such the Young's angle and contact-angle hysteresis also have influence on the detachment of droplets, especially critical voltage for droplet detachment. Achard and his coworkers[18,41] reported that a droplet sitting on the lower electrode in immiscible fluid can lift toward the upper substrate by electrostatic force, which is affected by the contact-angle hysteresis, especially the receding contact angle. For EW-driven detachment of droplets in air media, the threshold voltage for droplet detachment on superhydrophobic surfaces is smaller than that on hydrophobic surfaces due to lower contact-angle hysteresis of the superhydrophobic surfaces.[25] From these results, we can conjecture that similar situations can occur when an electrowetted droplet surrounded by oil media retracts and jumps on a solid surface with different contact-angle hysteresis.

We previously demonstrated that EW actuations with square-pulse signals can detach droplets in air from a hydrophobic surface.[25] In the present work, EW actuation with a single pulse signal is also employed to detach droplets in oil with high viscosity. The pulse width (T_p) is determined by measuring the spreading time (T_s), which is defined as the time elapsed to reach the peak of a spreading droplet under DC EW actuation (Fig. S7 in the

Supplementary Information). Here, the value of T_p is set to 17 ms regardless of applied voltage. The temporal variations of the base radius [Fig. 4(c)] and dimensionless height [Fig. 4(d)] are measured during the spreading, retracting, and jumping of droplets when a single pulse with different η is applied. Droplet jumping is observed when η is larger than 0.11, which corresponds to the applied voltage of 30 V. That is, when the droplet is actuated by EW with a single square pulse, the threshold voltage is decreased by 70% relative to the corresponding DC EW actuation. The maximum height of a jumping droplet actuated by EW with a single square pulse is about 1.5 times higher than that obtained by DC EW actuation. These results may arise from the fact that a droplet electrowetted with a square pulse voltage has a larger amount of surface energy than that with a DC voltage (Fig. S8 in the Supplementary Information). In addition, when a DC voltage is applied, an electrowetted droplet rests gently on the solid surface, before it starts to retract (i.e. afer the applied voltage is turned off). Therefore, the droplet velocity seems to be zero. However, when a square pulse voltage is applied, the droplet starts to retract as soon as it reaches to the maximum electrowetted radius. Thus, the droplet velocity is not zero. Consequently, when a DC voltage is applied, the surface energy is only converted to kinetic energy during retracting progress. On the other hand, when a square pulse voltage is applied, the sum of the surface energy and kinetic energy is converted into kinetic energy used for droplet detachment during retracting progress.

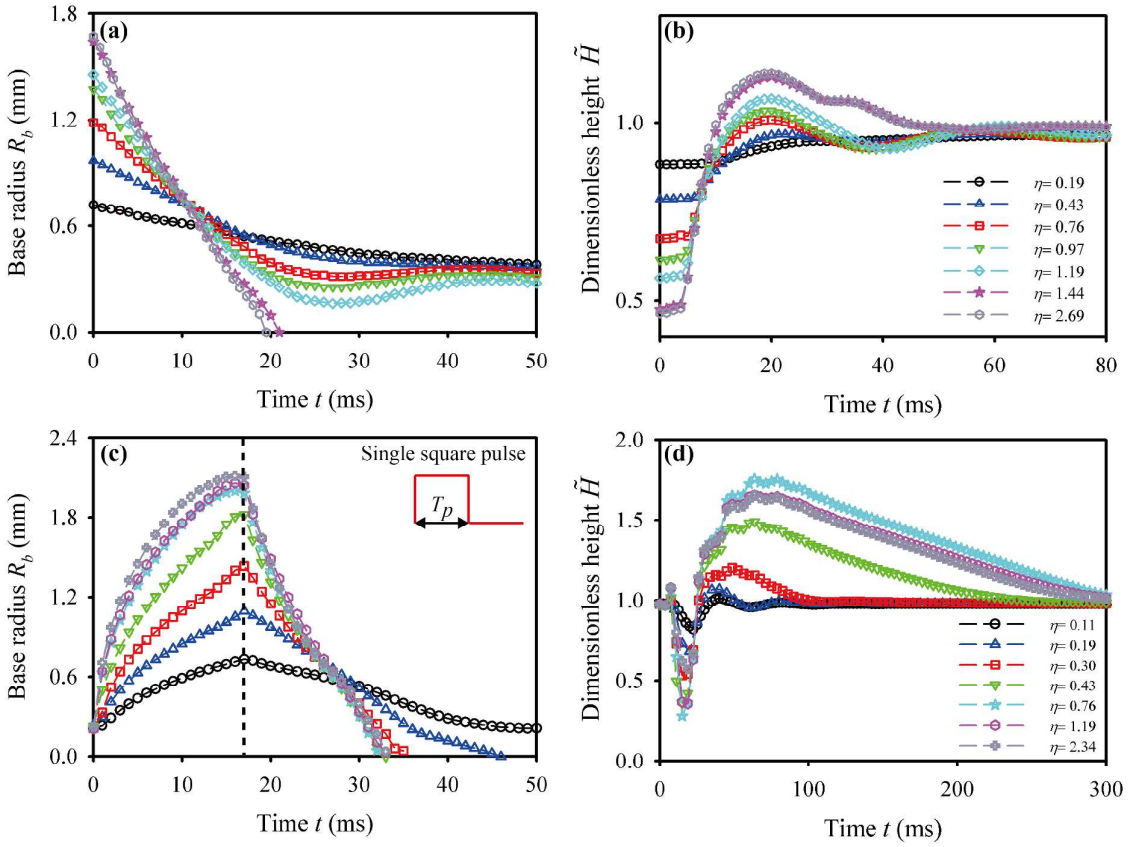

Fig. 4 Droplet detachment in silicone oil with high viscosity of 5cSt. (a) and (b) Temporal variations of base radius (R_b) and dimensionless height ($\tilde{H}$), respectively, of retracting and jumping of droplets at different EW numbers. (c) and (d) Temporal variations of base radius (R_b) and dimensionless height ($\tilde{H}$), respectively, during the spreading, retracting, and jumping processes of droplets under different EW actuations with a single square pulse. The inset in Fig. 3(c) depicts an electrical signal with a single square pulse. Here, the pulse width (T_p) is set to 17 ms regardless of applied voltage.

To get closer to the realization of a 3D-DMF platform for cell culture and cell-based assays, we preliminarily examine the detachment of 5μL droplets containing the mixture of

HUVECs and collagen (concentration of 4×10^4 cells/mL) in silicone oil with a viscosity of 0.65 cSt. These droplets electrowetted by a DC voltage cannot retract and jump due to adsorption of HUVECs and collagen on the solid surface. However, they can be easily detached from the solid surface without any residuals, when we apply electrical signals with square pulses with η= 1.2–2.7 at fixed T_p =15 ms, as shown in Fig. 5. Here, the T_p is determined by measuring the T_s for a 5 μL droplet containing a mixture of HUVECs and collagen (concentration of 4×10^4 cells/mL). The interfacial tension between the mixture and silicone oil is estimated to be about 0.023 N/m by using a public-domain image-processing program (ImageJ, NIH). To find the critical conditions of square pulse signals (e.g., the applied voltage and the pulse width) required for detaching droplets which contain biomaterials with different concentrations, further systematic study will be conducted in near future.

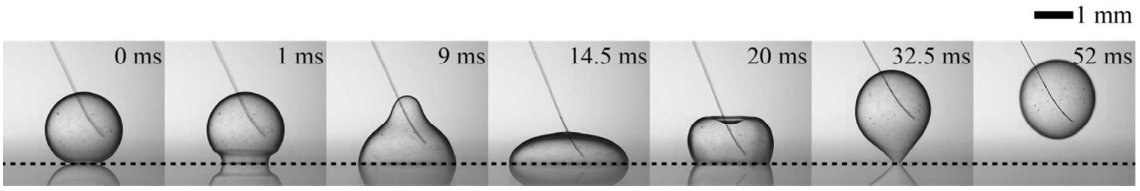

Fig. 5 Temporal shape variations of a detaching 5 μL droplet containing the mixture of human umbilical vein endothelial cells (HUVECs) and collagen (concentration of 4×10^4 cells/mL) in silicone oil with a viscosity of 0.65 cSt by applying a square pulse signal with η= 1.2 and T_p =15 ms.

On the other hand, the use of a needle electrode employed in the present work is somewhat limited in certain 3D-DMF platforms.[42] Compared to the needle electrode

configuration, a patterned electrode system can be easily integrated into lab-on-a-chip systems.[43,44] In addition, droplets are individually manipulated and basic fluidic operations, such as creating, transporting, splitting, and merging, can be performed on the patterned electrodes.[45] To complement the technical limitations in the use of a needle electrode, and to demonstrate the applicability of the 3D-DMF platform with patterned electrodes for chemical analysis and synthesis, we examine the transport, merging, mixing, and detachment of droplets with different pH values on the 3D-DMF platform with patterned electrodes (Fig. 6). The experimental apparatus is mainly consisted of two patterned electrode plates, which are combined with an acrylic cell, as shown in Fig. 6(a). Two droplets with the same volume of 3 μL are dispensed with a micropipette onto the bottom electrode plate. A droplet contains phosphate-buffered saline solution (Gibco) with 20 mM Na_2CO_3 (Sigma-Aldrich), which has a pH value of 8.6. The other droplet contains 0.2 mM phenol red (Sigma-Aldrich), which has a pH value of 5.3. The former and latter droplets exhibit colorless and yellow color, respectively. The materials and methods for this experiment are described in detail in the Supplementary Information.

First, a yellow-colored droplet (pH value of 5.3) is horizontally moved toward a colorless droplet (pH value of 8.6), and merged by sequentially applying a DC electrical signal with η= 1.3. Then, the two liquids inside the merged droplet are mixed by applying an AC electrical signal with η_{rms}= 1.3 at frequency of 20 Hz. During the mixing of the two liquids, the color of the merged droplet changes from yellow to red, because the pH value of the mixed solutions becomes 7.7. The phenol red used as a pH indicator displays red color in the range of pH value from 6.4 to 8.2. Subsequently, the droplet is vertically moved from the bottom to the upper electrode plate by retracting the electrowetted droplet at η= 5.6. Note that

the applied voltage is reduced to about 10% due to the presence of a 20 μm gap between the patterned electrodes, where electric voltage is not applied.[47] Finally, the droplet hanged on the upper electrode plate moves horizontally and vertically by employing the same strategies for horizontal and vertical transports of a droplet on the bottom electrode plate. To expand practical applications of the 3D-DMF platform with patterned electrodes, we are currently developing a droplet-manipulation platform and its chemical applications at high temperatures.

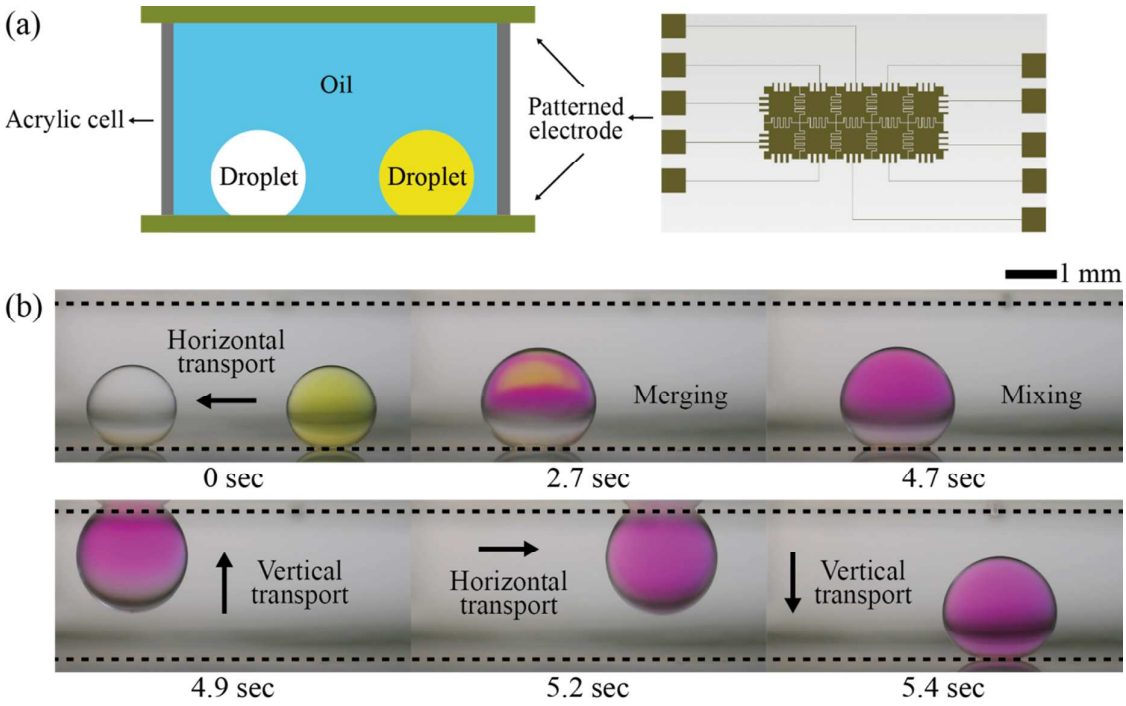

Fig. 6 (a) Schematic diagram of the experimental setup for three-dimensional digital microfluidics (3D-DMF) platform with patterned electrodes in oil. (b) Transport, merging, mixing, and detachment of two droplets with different pH values on the patterned electrodes by programmable control of electrical signals.

Oil droplets (e.g., silicone oil and dodecane) in water on a hydrophobic substrate have very low contact angle (< ~13°) and are thus difficult to detach from the solid surface. When DC voltage is applied to ambient water, water meniscus advances (or wets) on the hydrophobic surface, thus causing the oil droplet to retract [Fig. 7(a)]. When the contact radius of the oil droplet is sufficiently small, the oil–water interface becomes unstable, and the oil droplet is detached because of the contribution of buoyancy force. Residual droplets are occasionally observed on the solid surface after the detachment of the oil droplet because of the non-axisymmetric retracting motion of the oil droplet that results from its non-axisymmetric shape at the initial stage. Residual oil droplets can be detached by reapplying a DC voltage. From a practical viewpoint, AC EW actuation is employed to detach the oil droplet from a hydrophobic surface [Fig. 7(b)] because it has numerous advantages, including delay of contact-angle saturation,[48,49] decrease of contact-angle hysteresis,[50] and mixing enhancement.[51,52] The detailed study on the jumping conditions of oil droplets, such as oil type, droplet volume, and applied voltage, is beyond the scope of this research because consistently dispensing oil droplets with the same shape and volume is difficult.

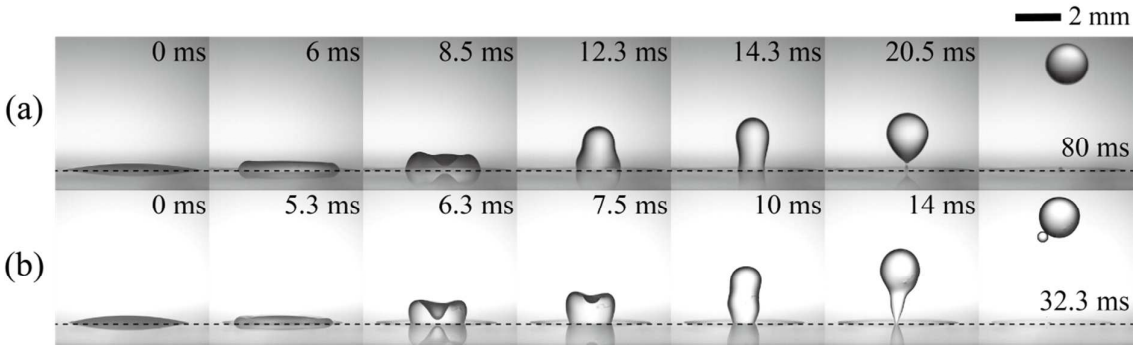

Fig. 7 Detachment of oil droplet in water. Transient shape deformation of a detaching 3 μL dodecane oil droplet in water under (a) DC EW actuation at EW number η = 1.41 and (b) AC EW actuation at EW number η_{rms} = 1.41 and frequency f = 10 Hz.

Conclusions

The detachment of sessile droplets submerged in immiscible fluids from a hydrophobic surface by EW was demonstrated. The critical conditions for droplet detachment are found as a function of physical parameters, including droplet volume, viscosity of ambient fluid, and applied voltage. When the droplet is actuated by EW with a single square pulse, the threshold voltage is reduced about 70% from that for the corresponding DC EW actuation. In addition, the maximum height of a jumping droplet actuated by EW with a single square pulse is about 1.5 times higher than that for the DC EW actuation. We demonstrate the detachment of droplets containing a mixture of HUVECs and collagen, which supports the applicability of development of 3D-DMF platforms to biological applications such as cell culture and cell-based assays. Furthermore, we examine the transport, merging, mixing, and detachment of droplets with different pH values on the 3D-DMF platform with patterned electrodes. This implies that the developed 3D-DMF platform with patterned electrodes can be used for chemical analysis and synthesis. Finally, both DC and AC EW actuations are observed to enable oil droplets in water to detach effectively from a hydrophobic surface.

Acknowledgement

This work was supported by the National Research Foundation of Korea (NRF) grant funded by the Korea government (MSIP) (No. 2008-0061991). The authors would also like to thank Mr. Young Kwon Kim and Ms. Eunseok Seo for their support on the experiments.

References

1. R. B. Fair, *Microfluid. Nanofluid.*, 2007, **3**, 245–281.

2. K. Choi, A. H. C. Ng, R. Fobel and A. R. Wheeler, *Annu. Rev. Anal. Chem.*, 2012, **5**, 413–440.

3. M. J. Jebrail, M. S. Bartsch and K. D. Patel, *Lab Chip*, 2012, **12**, 2452–2463.

4. J. El-Ali, P. K. Sorger and K. F. Jensen, *Nature*, 2006, **442**, 403–411

5. I. Barbulovic-Nad, H. Yang, P. S. Park and A. R. Wheeler, *Lab Chip*, 2008, **8**, 519–526.

6. H. Hufnagel, A. Huebner, C. Gulch, K. Guse, C. Abell and F. Hollfelder, *Lab Chip*, 2009, **9**, 1576–1582.

7. E. W. K. Young and D. J. Beebe, *Chem. Soc. Rev.*, 2010, **39**, 1036–1048 .

8. A. Ranella, M. Barberoglou, S. Bakogianni, C. Fotakis and E. Stratakis, *Acta Biomater.*, 2010, **6**, 2711–2720.

9. P. Y. Paik, K. Chakrabarty and V. K. Pamula, *IEEE Des. Test Comput.*, 2008, **25**, 372–381.

10. P. Y. Paik, V. K. Pamula and K. Chakrabarty, *IEEE Transactions on Very Large Scale Integration (VLSI) Systems*, 2008, **16**, 432–443.

11. Y. J. Zhao and S. K. Cho, *Lab Chip*, 2006, 6, 137–144.

12. Y. Zhao, S. K. Chung, U. C. Yi and S. K. Cho, *J. Micromech. Microeng.*, 2008, **18**, 1–11.

13. M. Jönsson-Niedziolka, F. Lapierre, Y. Coffinier, S. J. Parry, F. Zoueshtiagh, T. Foat, V. Thomy and R. Boukherroub, *Lab Chip*, 2011, **11**, 490–496.

14. A. James, B. Vukasinovic, M .K. Smith and A. Glezer, *J. Fluid Mech.*, 2003, **476**, 1–28.

15. H.-Y. Kim, *Phys. Fluids*, 2004, **16**, 474.

16. K. Takeda, A. Nakajima, K. Hashimoto and T. Watanabe, *Surf. Sci*., 2012, **519**, L589–L592**.**

17. J.-M. Roux, Y. Fouillet and J.-L. Achard, *Sens. Actuators A*, 2007, **134**, 486–493.

18. A. Glière, J.-M. Roux and J.-L. Achard, *Microfluid. Nanofluid*., 2013, **15**, 207–218.

19. D. T. Wasan and A. D. Nikolov, *Nature*, 2003, **423**, 156–159.

20. S. Wu, A. D. Nikolov and D. T. Wasan, *J. Colloid Interface Sci.*, 2013, **396**, 293–306.

21. F.-C. Wang and H.-A.Wu, *Soft Matter*, 2013, **9**, 7974–7980.

22. S. J. Lee, S. Lee and K. H. Kang, *J. Visual.*, 2011, **14**, 259–264.

23. S. J. Lee, S. Lee and K. H. Kang, *Appl. Phys. Lett.*, 2011, **100**, 081604.

24. F. Lapierre, Y. Coffinier, R. Boukherroub and V. Thomy, V. *Langmuir*, 2013, **29**, 13346−13351.

25. S. J. Lee, J. Hong, K. H. Kang, I. S. Kang and S. J. Lee, *Langmuir*, 2014, **30**, 1805−1811.

26. F. Mugele and J.-C. Baret, *J. Phys.: Condens. Matter*, 2005, **17**, R705−R774.

27. Y. Zhao and K. Chakrabarty, *IEEE Trans. Computer-Aided Design Integr. Circuits Syst.*, 2012, **31**, 817−830.

28. J.-Y. Yoon and R. L. Garrell, *Anal. Chem.*, 2013, **75**, 5097−5102.

29. M. G. Pollack, A. D. Shenderov and R. B. Fair, *Lab Chip*, 2002, **2**, 96–101.

30. H. Ren, R. B. Fair, M. G. Pollack and E. J. Shaughnessy, *Sens. Actuators B*,2002, **87**, 201–206.

31. W. C. Nelson, I. Peng, G.-A. Lee, J. A. Loo, R. L. Garrell and C.-J. Kim, *Anal. Chem.*, 2010, **82**, 9932–9937 (2010).

32. V. Srinivasan, V. K. Pamula and R. B. Fair, *Lab Chip*, 2004, **4**, 310–315.

33. V. Srinivasan, V. K. Pamula and R. B. Fair, *Anal. Chim. Acta*, 2004, **507**, 145–150.

34. J. Hong, Y. K. Kim, K. H. Kang, J. Kim and S. J. Lee, *Sens. Actuators B*, 2014, **196**, 292−297.

35. A. G. Banpurkar, K. P. Nichols and F. Mugele, *Langmuir*, 2008, **24**, 10549–10551.

36. P. Than, L. Preziosi, D. D. Josephl and M. Arney, *J. Colloid Interf. Sci.*, 1988, **124**, 552–559.

36. J. Hong, Y. K. Kim, K. H. Kang, J. M. Oh and I. S. Kang, *Langmuir*, 2013, **29**, 9118–9125.

37. B. M. Gillette, J. A. Jensen, B. Tang, G. J. Yang, A. Bazargan-Lari, M. Zhong and S. K. Sia, *Nat. Mater.*, 2008, **7**, 636–640.

38. E. Seo, K. W. Seo, J.-E. Gil, Y.-R. Ha, E. Yeom, S. Lee and S. J. Lee, *BMC Biotechnol.*, 2014, **14**, 61.

39. J. Hong, Y. K. Kim, K. H. Kang, J. Kim and S. J. Lee, *Sens. Actuators B*, 2014, **190**, 48–54.

40. D. Richard, C. Clanet and D. Quéré, *Nature*, 2002, **417**, 811.

41. J. M. Roux and J. L. Achard, *J. Electrostat.*, 2008, **66**, 283-293.

42. F. Mugele, A. Staicu, R. Bakker and D. van den Ende, *Lab Chip*, 2011, **11**, 2011–2016.

43. M. Abdelgawad, S.L.S. Freire, H. Yang and A.R. Wheeler, *Lab Chip*, 2008, **8**, 672–677.

44. L. Davoust, Y. Fouillet, R. Malk and J. Theisen, *Biomicrofluidics*, 2013, **7**, 044104.

45. S. K. Cho, H. J. Moon and C. J. Kim, *J. Microelectromech. Syst.*, 2003, **12**, 70–80.

46. D. J. Im, B. S. Yoo, M. M. Ahn, D. Moon and I. S. Kang, *Anal. Chem.*, 2013, **85**, 4038–4044.

47. U.-C. Yi and C.-J. Kim, *J. Micromech. Microeng.*, 2006, **16**, 2053−2059.

48. T. D. Blake, A. Clarke and E. H. Stattersfield, *Langmuir*, 2000, **16**, 2928–2935.

49. C. Quilliet and B. Berge, *Curr. Opin. Colloid Interface Sci.*, 2001, **6**, 34–39.

50. F. Li and F. Mugele, *Appl. Phys. Lett.*, 2008, **92**, 244108.

51. P. Paik, V. K. Pamula and R. B. Fair, *Lab Chip*, 2003, **3**, 253–259.

52. F. Mugele, J. C. Baret and D. Steinhauser, *Appl. Phys. Lett.*, 2009, **88**, 204106.